

The one-dimensional t-J model coupled to adiabatic phonons: A numerical investigation

Samuele Bissola¹ and Alberto Parola^{1,2}

¹ *Dipartimento di Fisica e Matematica, Università dell'Insubria, Via Valleggio 11 Como, Italy*

² *Istituto Nazionale per la Fisica della Materia, Como, Italy*

(Dated: March 23, 2022)

The ground state of the one-dimensional t-J model coupled with phonons in the adiabatic limit is numerically investigated by use of the Lanczos technique at quarter filling. Due to the interplay between the electron-electron Coulomb repulsion and electron-phonon interaction, this model shows a sequence of lattice distortions leading to the formation of charge-density-waves and bond-order-waves. Moderate electron-electron and electron-lattice coupling may lead to coexistence of dimerization and tetramerization in the distortion pattern. Dimerization leads to the formation of an “antiferromagnetic” Mott insulator, while tetramerization gives rise to a spin-Peierls phase. By increasing the super-exchange coupling, antiferromagnetism is inhibited due to the change of the distortion periodicity.

PACS numbers: 75.10.Jm 05.70.Jk 75.40.Cx

I. INTRODUCTION

In the last decades the physical and chemical properties of quasi one-dimensional (1D) systems have attracted growing attention due to the occurrence, in the same sample, of several different phases, ranging from insulating to superconducting, when a control parameter, like pressure, is varied^{1,2}. Inorganic compounds, as CuGeO_3 ³ or NaV_2O_5 ⁴, show clear evidence in favor of the existence of spin-Peierls states with broken lattice symmetry. Even more complex phase diagrams are displayed by quasi 1D organic materials: the $DI\text{--}DCNQI$ compounds^{5,6}, the Bechgaard salts series $(\text{TMTSF})_2X$ and its sulfur analog (Fabre salts series) $(\text{TMTTF})_2X$, where X denotes different monovalent anions ($X = \text{PF}_6, \text{AsF}_6, \text{ClO}_4, \dots$). These systems, which consist of stacks of weakly coupled chains, exhibit, at low temperature, several broken symmetry phases like charge-density-wave (CDW), spin-density-wave (SDW) and spin-Peierls (SP) before becoming superconducting^{6,7}. The physical mechanism underlying these strongly different orderings can be identified as the competition between lattice distortions and electron dynamics, with a major role played by electron interactions. Unfortunately, interaction effects in low dimensional electron systems coupled to further degrees of freedom, such as impurities or phonons, are not fully understood yet. Moreover, in order to describe the phase diagram of these materials the inclusion of inter-chain coupling besides interaction and phonons cannot be avoided. At the very least, inter-chain coupling is crucial for the stabilization of a genuine three dimensional long range order, like antiferromagnetism or superconductivity. However, we believe that, as a first step, a thorough understanding of the behavior of purely 1D strongly correlated electron systems coupled to adiabatic phonons is necessary.

By now, the physics of one dimensional electron systems in a rigid lattice is well understood⁸: spin isotropic models display a metallic phase, the celebrated Luttinger

Liquid (LL), with gapless charge and spin excitations. Umklapp processes occurring at commensurate fillings drive the opening of a charge gap, while attractive interactions may lead to pairing and then to a spin gap. The presence of a gapless branch of excitations is intimately related to the long range power law behavior of correlations and to the divergence of selected susceptibilities in these models. Remarkably, in 1D all these features are governed by a single parameter, denoted by K_ρ ⁸. In the LL phase both CDW and SDW susceptibilities at wave vector $q = 2k_F$ diverge for $K_\rho \leq 1$ while the CDW susceptibility at $q = 4k_F$ is singular for $K_\rho \leq 1/2$. Eventually, superconducting fluctuations become relevant for $K_\rho \geq 1$. The K_ρ parameter has been numerically evaluated as a function of the coupling constants in several 1D models⁸. If the Luttinger Liquid is weakly coupled to classical phonons, second order perturbation theory predicts the occurrence of lattice distortions of modulation q whenever the associated CDW susceptibility diverges.

In order to substantiate these perturbative results and to extend them to finite phonon coupling, the numerical study of simple lattice models on finite chains may indeed be profitable. The repulsive extended Hubbard model has been extensively investigated^{9,10,11,12,13} and the interplay between the $2k_F$ and $4k_F$ instabilities has been discussed. In such a class of models, the antiferromagnetic correlations are generated by virtual hopping processes and do not lead to an effective attraction between electrons. As a consequence, the key parameter K_ρ is restricted to the “repulsive” range $K_\rho \leq 1$. By contrast, in the t-J model the magnetic coupling J is unrelated to the on site repulsion ($U = \infty$) and K_ρ acquires values in the extended domain $1/2 \leq K_\rho < \infty$ ¹⁴. An investigation of the 1D t-J model coupled to adiabatic phonons would then allow to single out the role of antiferromagnetic fluctuations in driving lattice distortions and stabilizing CDW, SDW or SP ground states. This is the program we intend to pursue in the following sections.

II. THE MODEL

One of the simplest models able to describe the low energy properties of strongly correlated electron systems is the t-J model. Here, contrary to the Hubbard model, the magnetic interaction is explicitly included in the hamiltonian while the strong on site Coulomb repulsion acts via the single occupancy constraint. The phase diagram of the t-J model in a rigid 1D lattice has been determined¹⁴ and analytic solutions are known in the $J \rightarrow 0$ limit (spinless-fermion case)¹⁵ and at $J/t = 2$ (super-symmetric case)^{16,17}, besides at half filling, i.e. for electron density $n = 1$, where it reduces to the Heisenberg chain. In the latter case the model is known to be unstable toward dimerization (spin-Peierls instability) when coupled to an elastic lattice¹⁸. As a result, a periodic modulation of the lattice at wave-vector $q = 2k_F = \pi$ sets in and the system displays a bond-order wave (BOW): adjacent spins pair in a singlet state and a gap in the spin spectrum opens up. When phonons are treated in the adiabatic limit, this transition has been predicted for arbitrarily weak spin-lattice coupling¹⁸.

At finite doping, i.e. for electron density $n < 1$, the pure 1D t-J model enters the Luttinger Liquid phase which extends up to $J/t \lesssim 2.3$ (for $n = 1/2$) with growing superconducting fluctuations until, at larger J/t , phase separation sets in. Contrary to the purely repulsive Hubbard model, the t-J model explicitly exhibits the attraction mechanism between electrons mediated by antiferromagnetic fluctuations which is likely to be present in real magnetic materials.

In the following, we study 1D t-J model coupled with classical phonons and we investigate by numerical diagonalization technique the interplay between electron interactions and lattice distortions. We focus our attention on the competition, or sometimes the cooperative behavior, between charge ordering and lattice instabilities and we examine its consequences on the magnetic properties of the materials. The calculations will be performed at quarter filling ($n = 1/2$), which is the appropriate choice to mimic the behavior of the organic compounds⁶, and our results are summarized in Fig. 1 which shows a tentative zero temperature phase diagram of the model.

The one-dimensional t-J model coupled with adiabatically phonons is defined by the hamiltonian

$$\begin{aligned}
 H = & - \sum_i (1 - \delta_i) \left(\tilde{c}_{i,\sigma}^\dagger \tilde{c}_{i+1,\sigma} + h.c. \right) + \\
 & + J \sum_i (1 - \delta_i) \left(\mathbf{S}_i \cdot \mathbf{S}_{i+1} - \frac{1}{4} n_i n_{i+1} \right) + \\
 & + \frac{1}{2} K_B \sum_i \delta_i^2
 \end{aligned} \quad (1)$$

Where \mathbf{S}_i are spin-1/2 operators at the site i , $\tilde{c}_{i,\sigma}^\dagger = c_{i,\sigma}^\dagger (1 - n_{i,-\sigma})$ are electron Gutzwiller-projected creation operators and $n_i = \sum_\sigma c_{i,\sigma}^\dagger c_{i,\sigma}$. We have also set

the bare hopping integral t to unity thereby fixing the energy scale. The hamiltonian depends on the classical variables δ_i which identify the bond distortions defined as $\delta_i = (u_{i+1} - u_i)$ where u_i is the displacement of ion i with respect to its equilibrium position. The last contribution represents the elastic deformation energy and K_B is the spring constant. The form of the electron-phonon coupling adopted here follows from a linearization of the expected dependence of the coupling constants on lattice distortions: for small displacements δ of the ion sites, the hopping and exchange integrals vary with the distance as a certain power¹⁹ α which has been estimated in the range $6 < \alpha < 14$

$$J_{i,i+1}(\delta) = J \left(\frac{a + u_i}{a + u_{i+1}} \right)^\alpha \simeq J \left(1 - \alpha \frac{\delta}{a} \right)$$

where a is the bare lattice spacing. For simplicity we have taken the same α for both the hopping and the super-exchange integrals. We note that the Hamiltonian (1) is invariant under the rescaling $\alpha \rightarrow \lambda \alpha^*$, $K_B \rightarrow \lambda^2 K_B^*$, $\delta \rightarrow \delta^*/\lambda$, where λ is the rescaling factor. We can then fix one parameter between α and K_B ²⁰ without affecting the physics of the model. In the hamiltonian (1) we have set $\alpha = 1$. Clearly, the physical range where the hamiltonian (1) may be used is restricted to $|\delta_i| \ll 1$.

This model is studied at quarter filling ($n = 1/2$) and zero magnetization by use of the Lanczos method on a finite ring 16 sites. Contrary to previous studies on the Hubbard model, we choose open shell boundary conditions, i.e. periodic boundary conditions when the number of lattice sites L is an integer multiple of 8, anti-periodic boundary conditions otherwise. This choice is motivated by the attempt to mimic the behavior of an infinite chain in a small ring. As already noticed, a key feature of the t-J model in the thermodynamic limit is the presence of gapless excitations which lead to a diverging CDW susceptibility, and then to lattice distortions. In closed shell rings, this feature is lost because of the $O(1/L)$ finite size gap in the kinetic energy spectrum. As a consequence, unrealistically low values of the elastic constant K_B are needed in order to stabilize lattice distortions¹².

The ground state of the hamiltonian (1) is numerically obtained by Lanczos technique at fixed $\{\delta_i\}$. The lattice distortions are then updated in order to minimize the total energy $E(\{\delta_i\})$. This can be accomplished by solving the self-consistency equations which follow from the Hellmann-Feynman theorem:

$$\begin{aligned}
 \frac{\partial E}{\partial \delta_i} = & \sum_\sigma \langle \tilde{c}_{i,\sigma}^\dagger \tilde{c}_{i+1,\sigma} + h.c. \rangle + J \langle S_i \cdot S_{i+1} - \frac{1}{4} n_i n_{i+1} \rangle \\
 & + K_B \delta_i + \frac{1}{N} \sum_{j,\sigma} \langle \tilde{c}_{j,\sigma}^\dagger \tilde{c}_{j+1,\sigma} + h.c. \rangle - \\
 & - \frac{J}{N} \sum_j \langle S_j \cdot S_{j+1} - \frac{1}{4} n_j n_{j+1} \rangle = 0
 \end{aligned} \quad (2)$$

The constraint $\sum_i \delta_i = 0$ which reflects the chosen ring geometry has been implemented by use of a Lagrange

multiplier. Here $\langle \dots \rangle$ is the ground-state expectation value. In order to find the bond length configuration which minimizes the total energy at given coupling constants (J, K_B) we iterate the set of equations (2) until convergence is reached.

III. NUMERICAL RESULTS

Here we present the numerical results on the t-J model coupled to adiabatic phonons at quarter filling and vanishing magnetization for a 16 site ring. In this case $k_F = n\pi/2 = \pi/4$ and the two expected, competing periodicities correspond to tetramerization ($q = 2k_F$) and dimerization ($q = 4k_F$). In the former case two electrons belong to the unit cell and then we expect a paramagnetic insulator behavior with both charge and spin gap. This regime precisely corresponds to the spin-Peierls phase experimentally found in the Fabre salt series. Instead, in the presence of lattice dimerization, the model should be a paramagnetic metal, having a single electron per unit cell. However, the residual Coulomb repulsion drives the system toward a Mott insulator phase. Such a circumstance can be explicitly checked in the $J \rightarrow 0$ limit, where some exact statement can be made.

In one dimension, when the kinetic term alone is present, the charge degrees of freedom are described by a free spinless fermion gas¹⁵ whose properties, even in the presence of (adiabatic) phonon coupling, can be explicitly derived in the thermodynamic limit. Lattice dimerization is stabilized for arbitrarily large K_B ²¹ but such a symmetry breaking cannot be accompanied by a CDW of the same periodicity because reflection across a bond leaves the distortion pattern unaltered while interchanging the two sublattices. As a result, in the t-J model at $n = 1/2$ and $J \rightarrow 0$, the charge distribution remains uniform along the chain while a charge gap opens due to the doubling of the unit cell. The spin degrees of freedom arrange as in the ground state of the Heisenberg chain and the spin correlations can be expressed in a factorized form²²:

$$\langle \mathbf{S}_r \cdot \mathbf{S}_0 \rangle = \sum_{j=2}^{r+1} P_{SF}^r(j) S_H(j-1) \quad (3)$$

where $P_{SF}^r(j)$ is the probability of finding j particles in $(0, r)$ with one particle in 0 and another in r , evaluated in the ground state of the dimerized spinless Fermi gas. If we set $N_r = \sum_{i=0}^r n_i$, the probability $P_{SF}^r(j)$ can be formally expressed as $P_{SF}^r(j) = \langle n_0 n_r \delta(N_r - j) \rangle$ and $S_H(j) = \langle \mathbf{S}_j \cdot \mathbf{S}_0 \rangle_H$ is the spin-spin correlation function of the isotropic Heisenberg chain. Following Ref.²² the asymptotic decay of Eq. (3) in the presence of lattice dimerization can be evaluated as

$$\langle \mathbf{S}_r \cdot \mathbf{S}_0 \rangle \propto \frac{\cos(2k_F r - \frac{\pi}{4})}{r} \quad (4)$$

much slower than in the standard t-J model at the same electron density. This asymptotic result valid for any

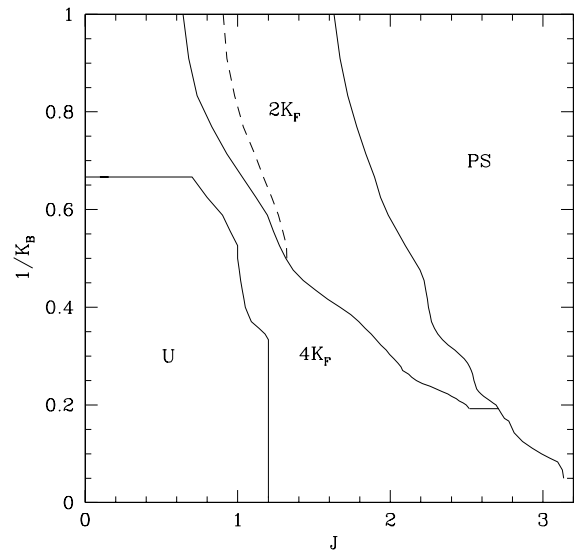


FIG. 1: Phase diagram of the t-J model coupled to adiabatic phonons (1) obtained by numerical diagonalization of a 16 site chain. The boundaries of the uniform phase (U), the dimerized BOW ($4k_F$), the tetramerized BCDW ($2k_F$) and the phase separated region are shown by full lines. The dashed line represents a crossover between the bond pattern shown in Figs. 2c (left) and 2d (right).

lattice dimerization, can be understood from Eq. (3) in the simpler limit of decoupled dimers, i.e for $\delta_i \sim (-1)^{i+1}$ where

$$P_{SF}^r(j) = \frac{1}{4} \cdot \begin{cases} 0 & \text{for } r = 1 \\ \delta_{j, (r+1)/2} & \text{for } r \text{ odd} \neq 1 \\ \delta_{j, (r+2)/2} & \text{for } r \text{ even} \end{cases} \quad (5)$$

Remarkably, Eq. (4) reproduces the same $1/r$ decay of spin correlations as in the usual Heisenberg chain. This form of the magnetic correlations, together with the presence of a charge gap shows that the model is indeed in a Mott insulator phase. Such a result suggests that lattice dimerization strongly favors antiferromagnetism, which will be eventually stabilized by inter-chain coupling giving rise to three dimensional antiferromagnetic ordering. Therefore, in the $J \rightarrow 0$ limit, the t-J model coupled to adiabatic phonons reproduces one of the phases experimentally found in the quasi one dimensional Fabre salts. Now we want to investigate how the enhancement of antiferromagnetic coupling induced by the J term modifies this picture.

The numerical results are summarized in Fig. 1 where the phase diagram emerging from our analysis is sketched. No lattice or spin symmetry has been imposed and the Lanczos diagonalization has been performed in the full Hilbert space of the model. This strongly limits the feasible sizes to the range $L \leq 16$. In all cases the ground state we found shows definite lattice periodicity, the result does not depend on the starting bond configuration or on the convergence requirements. Noticeable

exceptions to this statement are the states in the phase separated region (PS in Fig. 1) at very large J , where the energy landscape presents several local minima. In order to check the stability of the numerical results, we performed a set of Lanczos diagonalizations in the reduced Hilbert space obtained by selecting a given unit cell (e.g. two sites or four sites). We always found consistency between the numerical output in the full and in the reduced Hilbert space except in the PS region, where the ground state energy obtained in every subspace of definite translational symmetry is larger than the ground state energy found in the full Hilbert space. This feature identifies the boundary of the PS region. We will not discuss this unphysical regime any further.

The distortion patterns we found correspond to periodicities of growing wavelength moving from small J to larger J :

- uniform (U in Fig. 1)
- dimerized ($4k_F$ in Fig. 1)
- tetramerized ($2k_F$ in Fig. 1)

A general feature of the phase diagram we obtained is the rather weak dependence of the phase boundaries on the spring constant K_B : this shows that the antiferromagnetic coupling J is indeed the driving force which selects the periodicity of lattice distortions. In the uniform phase, $\delta_i = 0$ and the system is a metal according to the theory of Luttinger Liquids. The numerical data predict a uniform phase also in the previously discussed $J \rightarrow 0$ and large K_B limit where the charge degrees of freedom behave as spinless fermions which are known to undergo spontaneous dimerization when coupled to adiabatic phonons. This shows that, at least in this region, strong finite size effects are present in our small cluster. In order to investigate this problem, we performed few Lanczos diagonalizations for the $L = 20$ site chain in the Hilbert sub-space defined by the eigenstates of the four site translation operator. This calculation allows to study the interplay between uniform solution, dimerization and tetramerization in this cluster. The phase boundary between the uniform and the dimerized phase shrinks from $J \sim 1.2$ to $J \sim 0.8$ at $K_B = 3$ while the onset of tetramerization hardly moves. Therefore we are led to conclude that, as already discussed in previous numerical studies of the Hubbard model¹¹, the very existence of the uniform phase in the adiabatic limit is likely to be an artifact of the smallness of the cluster considered, while the other phase are much less affected by finite size problems.

At larger J the dimerized $4k_F$ state prevails and according to the previous analysis the chain behaves as a Mott insulator. While the electron density remains uniform, the lattice develops a bond ordered wave (BOW): a charge gap opens due to the Umklapp processes triggered by the doubling of the unit cell and the cell-cell spin correlations show an extremely slow decay characterized by

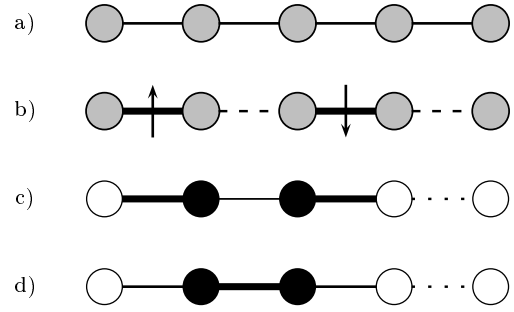


FIG. 2: Pictures of the competing density waves in the ground state. a) Uniform state (U), b) $4k_F$ BOW and uniform charge, c) $2k_F$ BCDW tetramerized phase ($S - W - S - W'$), d) $2k_F$ BCDW tetramerized phase ($U - S - U - W$).

a diverging antiferromagnetic susceptibility. When three dimensional coupling is allowed for, a genuine antiferromagnetic long range order sets in.

Finally, by further increasing J , the lattice periodicity changes and the unit cell doubles again giving rise to lattice tetramerization. In this case, a weak $2k_F = \pi/2$ charge density wave develops on top of the lattice distortion giving rise to a bond/charge density wave (BCDW)^{10,11}:

$$\begin{aligned} \langle n_i \rangle &= \frac{1}{2} + A_{2k_F} \cos\left(\frac{\pi}{2}i + \frac{\pi}{4}\right) \\ \delta_i &= B_{4k_F} \cos(\pi i) + B_{2k_F} \cos\left(\frac{\pi}{2}i\right) \end{aligned} \quad (6)$$

The phase shifts shown in Eq.(6) are those obtained by the numerical diagonalization and correspond to a CDW of the type $-++-$, where $+$ ($-$) identifies a local density higher (lower) than the average ($n = 1/2$). No significant $4k_F$ component in the CDW is detected in the BCDW, in agreement with previous investigations of the Hubbard model. Interestingly, the bond pattern depends on the relative magnitude of the B_{4k_F} and B_{2k_F} amplitudes: For $B_{4k_F} > |B_{2k_F}|$ the ordering is of the type $S - W - S - W'$ (Fig. 2c) while for $|B_{4k_F}| < B_{2k_F}$ the sequence is $U - S - U - W$ (Fig. 2d). Here, W , U and S respectively represent a weak (W) almost undistorted (U) and strong (S) bond. Although no real transition, but rather a crossover, is present between these two cases, we can identify a small region (shown in Fig. 1) where the bond ordering is of the first type, while in the remaining region of stability of the tetramerized phase the bond lengths arrange as in Fig. 2d. The crossover between these two different realizations of the $2k_F$ phase may be understood by noting that the $S - W - S - W'$ BOW (Fig. 2c) appears as an intermediate regime between the $4k_F$ region and the stable $U - S - U - W$ (Fig. 2d) ordering, which indeed dominates in a large portion of the phase diagram.

Notice that previous studies of the extended Hubbard model^{11,12} found only a pattern of the first type, which is

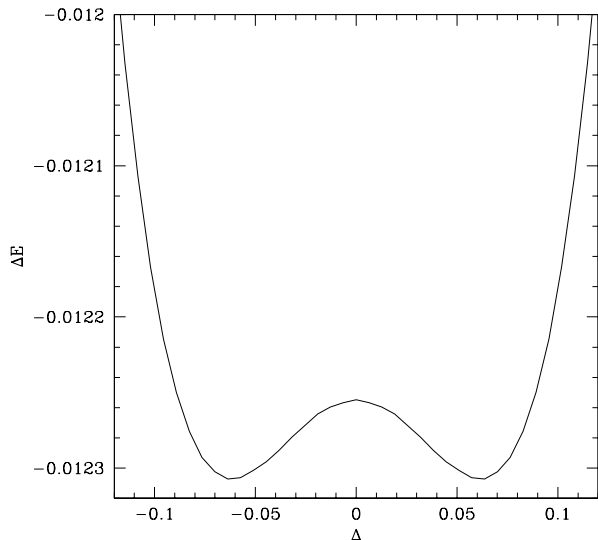


FIG. 3: Energy landscape at $J = 0.7$ and $K_B = 1$. The ground state energy, referred to the undistorted state, is plotted as a function of the difference Δ between the two weak bonds in the $S - W - S - W'$ phase. The strong bond is fixed at the equilibrium value $\delta = 0.15925$

often referred to as the dimerization of an already dimerized state. In such a regime, our calculations suggest the occurrence of a transition between a low temperature tetramerized phase and dimerization at higher temperature. In order to investigate this possibility, which is indeed experimentally found in *DI - DCNQI* compounds, we evaluated the ground state energy of the 16 site ring at given lattice distortion: We kept the amplitude of the two strong bonds fixed while varying the difference Δ between the two weak bonds of the unit cell $S - W - S - W'$. The result, shown in Fig. 3 for $J = 0.7$ and $K_B = 1$, displays a double well structure characterized by a small energy barrier between the tetramerized ground state at $\Delta \sim \pm 0.06$ and the dimerized configuration corresponding to $\Delta = 0$.

Whenever lattice tetramerization prevails, two electrons belong to the unit cell and then the chain becomes a paramagnetic band insulator as in the spin-Peierls phase. We believe that, because of the presence of both charge and spin gap, this phase is stable toward 3D coupling.

It is interesting to investigate the energy difference between the electronic states corresponding to the low energy lattice distortions which are solutions of Eq. (2). Such a calculation may provide some useful information about the temperature range where an ordered phase is indeed stable. In Fig. 4 we plot the energy of different distortions as a function of J at fixed $K_B = 3$. More precisely, we plot the energy difference between the lowest metastable state of a given periodicity ($4k_F$ or $2k_F$) and the uniform solution.

The numerical data also suggest first order boundaries between the uniform and the dimerized phase, as can be inferred by the sudden jump of the appropriate Fourier

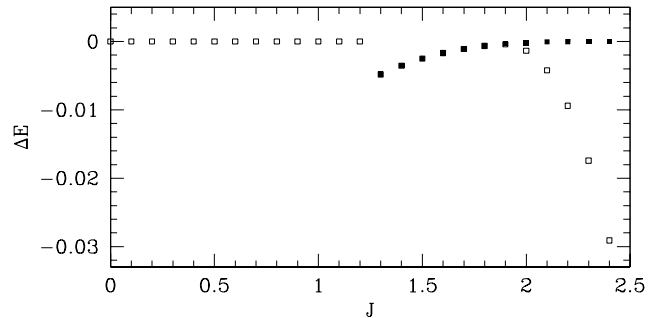


FIG. 4: Energy gains between different distortions at fixed $K_B = 3$ in a $L = 16$ site ring. Open (full) squares refer to a four (two) site unit cell.

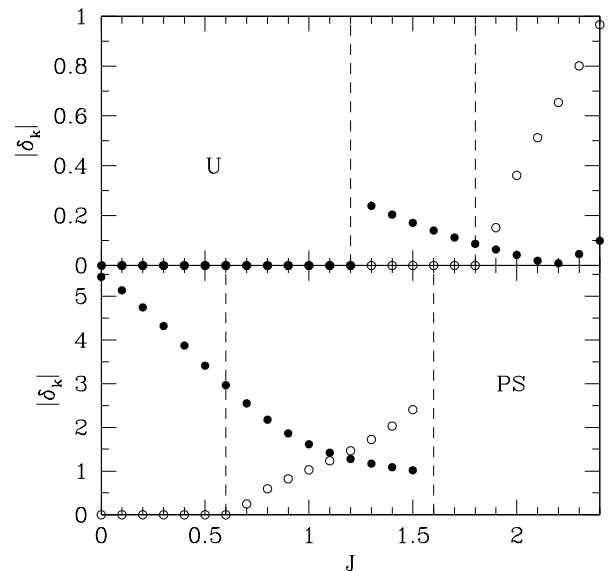


FIG. 5: Amplitude of the $4k_F$ (full dots) and $2k_F$ (open dots) Fourier components of the bond distortions in the ground state of the model. Upper panel: $K_B = 3$, lower panel $K_B = 1$

component of the lattice distortion $\{\delta_i\}$ shown in Fig. 5 for a couple of values of K_B . Our results do not allow to draw any definite conclusion about the order of the transition between the dimerized and the tetramerized phase.

Although the periodicities of the lattice distortions we found numerically precisely correspond to those expected on the basis of the instabilities of the homogeneous t-J model, some discrepancy on the sequence of distortion patterns does occur. As previously discussed, the t-J model is characterized by a K_ρ parameter always larger than $1/2$ in the whole range $J > 0$. This would imply that, at least in the perturbative regime of small distortions (i.e. for $K_B \rightarrow \infty$), pure dimerization should never be observed. Instead, tetramerization should be seen for $0 < J \lesssim 2.3$ which, according to Ref.¹⁴, corresponds to $K_\rho \leq 1$. While the upper limit for $2k_F$ distortions

roughly agrees with the Lanczos diagonalization data, the numerical results clearly show that, for large K_B , dimerization and not tetramerization provides the most stable distortion pattern. This behavior can be understood by noting that the *amplitude* of the $2k_F$ singularity in the charge response of the uniform t-J model is strongly suppressed for $J \lesssim 2$, as already noted in Refs.^{24,25}. This suggests that even if in the thermodynamic limit a $2k_F$ singularity may eventually prevail in the whole phase diagram, at small J a clear *dimerization* pattern with only weak tetramerization corrections will be visible.

IV. CONCLUSIONS

In summary, we determined the phase diagram of the 1D t-J model adiabatically coupled to the lattice by use of Lanczos diagonalization in small clusters. We found, for increasing antiferromagnetic coupling, a metallic uniform phase, a BOW phase which displays the typical features of a Mott insulator and preludes to 3D antiferromagnetic (AF) order, a BCDW phase which realizes the spin-Peierls scenario. Therefore, by *increasing* the AF coupling J in the model the systems goes from antiferromagnetic to paramagnetic because of the change in distortion pattern determined by the charge degrees of freedom. This shows that in the t-J model charge and spin ordering compete due to the coupling to the lattice

and strong super-exchange interaction may lead to a spin-Peierls ground state. Remarkably, the phases we found are all present in the typical zero temperature phase diagram of the quasi 1D organic materials⁷. Moreover, these phases do indeed occur in the same sequence as we found when uniform pressure is applied to the material. The effect of pressure is mainly to increase the hopping amplitude (which we set as unit of energy) and then our results are compatible with the experiments provided the effective intra-chain superexchange coupling J is only weakly dependent on the applied pressure. If this is the case, the t-J model may indeed represent a useful theoretical framework for the interpretation of the behavior of the quasi 1D organic materials.

The effects of charge ordering in this class of materials has been mainly investigated by using an extended Hubbard model coupled with the lattice^{11,12}. A phase diagram, of the ground state, obtained as a function of the electron-phonon couplings show the same periodicities that we found with the exception of the one in Fig. 2d. Notice that the strong coupling limit of the extended Hubbard model is related to an effective t-J model²⁷ by $J = \frac{4t^2}{U-V}$, which restricts the mapping to the $J \ll 1$ regime.

It is a pleasure to thank F. Becca for stimulating discussions. Financial support by the MIUR-PRIN program is gratefully acknowledged.

-
- ¹ C. Bourbonnais, and D. Jerome, (cond-mat 9903101) *Advances in Synthetic Metals, Twenty years of Progress in Science and Technology* (Elsevier, New York, 1999), pp. 206-301.
 - ² H. Wilhelm, D. Jaccard, R. Duprat, C. Bourbonnais, D. Jerome, J. Moser, C. Carcel, and J.M. Fabre, Eur. Phys. J. B **21**, 175 (2001).
 - ³ M. Hase, I. Terasaki, and K. Uchinokura, Phys. Rev. Lett. **70**, 3651 (1993).
 - ⁴ D. Smirnov, P. Millet, J. Leotin, D. Poilblanc, J. Riera, D. Augier, and P. Hansen, Phys. Rev. B **57**, R11035 (1998).
 - ⁵ M. Meneghetti, C. Pecile, K. Yakushi, K. Yamamoto, K. Kanoda, and K. Hiraki, Solid State Chem. **168**, 632 (1999).
 - ⁶ M. Dumm, A. Loidl, B.W. Fravel, K.P. Starkey, L.K. Montgomery, and M. Dressel, Phys. Rev. B **61**, 511 (2000).
 - ⁷ D. Jerome, Science **252**, 1509 (1991).
 - ⁸ H.J.Schulz, G. Cuniberti, and P. Pieri, *Field Theories for Low-Dimensional Condensed Matter Systems* (Springer, 2000).
 - ⁹ S. Mazumdar, S.N. Dixit, and A.N. Bloch, Phys. Rev. B **30**, R4842 (1984).
 - ¹⁰ K.C. Ung, S. Mazumdar, and D. Toussaint, Phys. Rev. Lett. **73**, 2603 (1994).
 - ¹¹ R.T. Clay, S. Mazumdar, and D.K. Campbell, Phys. Rev. B **67**, 115121 (2003).
 - ¹² J. Riera, and D. Poilblanc, Phys. Rev. B **62**, R16243 (2000).
 - ¹³ M. Kuwabara, H.Seo, and M. Ogata, J. Phys. Soc. Jpn. **72**, 225 (2003).
 - ¹⁴ M. Ogata, M. U. Luchini, S. Sorella, and F. F. Assaad, Phys. Rev. Lett. **66**, 2388 (1991).
 - ¹⁵ M.Ogata and H. Shiba, Phys. Rev. B **41**, 2326 (1990).
 - ¹⁶ P.A. Bares, and G. Blatter, Phys. Rev. Lett. **64**, 2567 (1990).
 - ¹⁷ P.A. Bares, G. Blatter, and M. Ogata, Phys. Rev. B **44**, 130 (1991).
 - ¹⁸ M.C. Cross, and D.S. Fisher, Phys. Rev. B **19**, 402 (1979).
 - ¹⁹ W.A. Harrison, *Electronic structure and the properties of solids* (Dover, New York, 1980).
 - ²⁰ F. Becca, and F. Mila, Phys. Rev. Lett. **89**, 037204 (2002).
 - ²¹ R.E. Peierls, *Quantum theory of Solids* (Oxford, 1955).
 - ²² A. Parola, and S. Sorella, Phys. Rev. Lett. **64**, 1831 (1990).
 - ²³ R.J. Bursill, R.H. McKenzie, and C.J. Hamer, Phys. Rev. Lett. **83**, 408 (1999).
 - ²⁴ F.F. Assaad, and D. Wurtz, Phys. Rev. B **44**, 2681 (1991).
 - ²⁵ M. Troyer, H. Tsunetsugu, T.M. Rice, J. Riera, and E. Dagotto, Phys. Rev. B **48**, 4002 (1993).
 - ²⁶ Y. Nakazawa, A. Sato, M. Seki, K. Saito, K.I. Hiraki, T. Takahashi, K. Kanoda, and M. Sorai, Phys. Rev. B **68**, 085112 (2003).
 - ²⁷ J. van den Brink, M.B.J. Meinders, J. Lorenzana, R. Eder, and G. A. Sawatzky, Phys. Rev. Lett. **75**, 4658 (1995).